01 Apr 2008

Natrolitite, an Unusual Rock -- Occurrence and Petrographic and Geochemical Characteristics (Eastern Turkey)

Emin Ciftci

John Patrick Hogan
Missouri University of Science and Technology, jhogan@mst.edu

Hasan Kolayli

Emin Cadirli

Recommended Citation

NATROLITITE, AN UNUSUAL ROCK – OCCURRENCE AND PETROGRAPHIC AND GEOCHEMICAL CHARACTERISTICS (EASTERN TURKEY)

EMIN ÇIFTÇI[1],*, JOHN P. HOGAN[2], HASAN KOLAYLI[3], AND EMIN ÇADIRLI[4]

[1] Department of Geological Engineering, Nigde University, 51245 Nigde, Turkey
[2] Department of Geology and Geophysics, University of Missouri-Rolla, Rolla, MO 65401, USA
[3] Department of Geological Engineering, Karadeniz Technical University, 61200 Trabzon, Turkey
[4] Department of Physics, Nigde University, 51245 Nigde, Turkey

Abstract—Very unusual rocks consisting of natrolite (>95 vol.%) ± pargasite (<5 vol.%) and rare albite (<1 vol. %) have been discovered in the Kop mountain range, eastern Turkey. We propose to call these rocks 'natrolitite' and 'pargasite natrolitite'. They were produced by Na Si metasomatism of dikes and stocks of diorite through replacement of the intermediate primary igneous plagioclase to produce natrolite. The metasomatic alteration produced concentric elliptical zones characterized by distinct mineral assemblages centered on intrusions of diorite. The Central Zone 1 consists of variably albitized diorite with preserved magmatic textures (albite ± andesine ± pargasite ± quartz). Transition Zone 2 comprises natrolite-bearing diorite (natrolite ± albite ± andesine ± pargasite ± calcite ± quartz). Marginal Zone 3 is a rock made up almost entirely of natrolite (natrolite ± pargasite ± albite ± calcite ± chlorite). Outer Zone 4 occurs along the boundary between the natrolitite and the surrounding serpentinite and consists of listvenite, a rock which comprises magnesite, quartz, calcite, mica, talc, and hematite, indicating a role for CO_2 in the metasomatic reactions, consistent with the presence of calcite in the alteration zones. Zone 5 consists essentially of brecciated serpentinite with numerous hydrothermal quartz veins and calcite veins. Whole-rock compositions document an increase in Na_2O, Al_2O_3, and H_2O from the core (central zone) to the margin while CaO, MgO, and SiO_2 decrease. Plagioclase abundance and composition also varies outwards from the central core rocks where it occurs as a primary magmatic phase (~95 vol.% An_{41-38}) to the alteration zones (<5 vol.% An_{32-37}) due to partial to complete replacement of plagioclase by natrolite with or without rare albite. The natrolites exhibit little variation in Si/Al ratios, ranging between 1.45 and 1.61, and are similar in composition to those reported in the literature. Accompanying pargasitic amphibole also becomes progressively more sodic in composition from the core rocks to the marginal zone rocks. Our analysis indicates that albitization preceded the formation of natrolite and that the formation of natrolite, instead of other more typical alteration minerals (*e.g.* analcime and paragonite), reflects Na metasomatism at lower chemical potentials for Al_2O_3 and SiO_2. Potential sources of Na could be hypersaline brines or leaching of country rocks, such as trondhjemites. The fluids were driven in hydrothermal convection cells set up by the intrusion of the diorites.

Key Words—Eastern Turkey, Kop Mountains, Listvenite, Metasomatism, Natrolite, Natrolitite, Pargasite, Zeolites.

INTRODUCTION

Zeolites are well known worldwide as important, mainly secondary, rock-forming minerals. They typically occur in igneous rocks, particularly basaltic flows, as fracture fillings and amygdales (Graham *et al.*, 2003; Utada, 2001a; Langella *et al.*, 2001; Sheppard and Hay, 2001a; Lo and Song, 2000; Filippidis *et al.*, 1996; Ibrahim and Hall, 1996; Teertstra and Dyer, 1994; Gunter *et al.*, 1993; Flohr and Ross, 1990; Vattuone de Ponti and Latorre, 1990; Rouse *et al.*, 1990; Arzamastsev *et al.*, 2000). They also commonly occur as authigenic silicate minerals in sedimentary rocks (Sheppard and Hay, 2001b). Zeolites form from a variety of precursor minerals including volcanic and impact glasses, aluminosilicate gels, and aluminosilicate minerals, including other zeolites, kaolinite, smectite, feldspars, and feldspathoids, during burial diagenesis and low-grade metamorphism (Utada, 2001b).

This paper reports the occurrence of a very unusual rock type, consisting of >95% of the zeolite natrolite, a hydrated sodium aluminum framework silicate ($Na_2[Al_2Si_3O_{10}]\cdot 2H_2O$), with or without minor amounts of the pargasitic amphibole and albite from the Kop mountains of eastern Anatolia in Turkey. Many of the diorites retain nearly pristine igneous textures in thin section, as the natrolitization process has preserved the primary plagioclase morphology. Thus, the true nature of these rocks remained undiscovered until X-ray diffraction data revealed the 'plagioclase' that was thought to be present in these rocks is instead essentially all natrolite. To our knowledge this is the first report of such rocks in the literature. Thus, we propose naming such rocks 'natrolitite' and 'pargasite natrolitite'. The
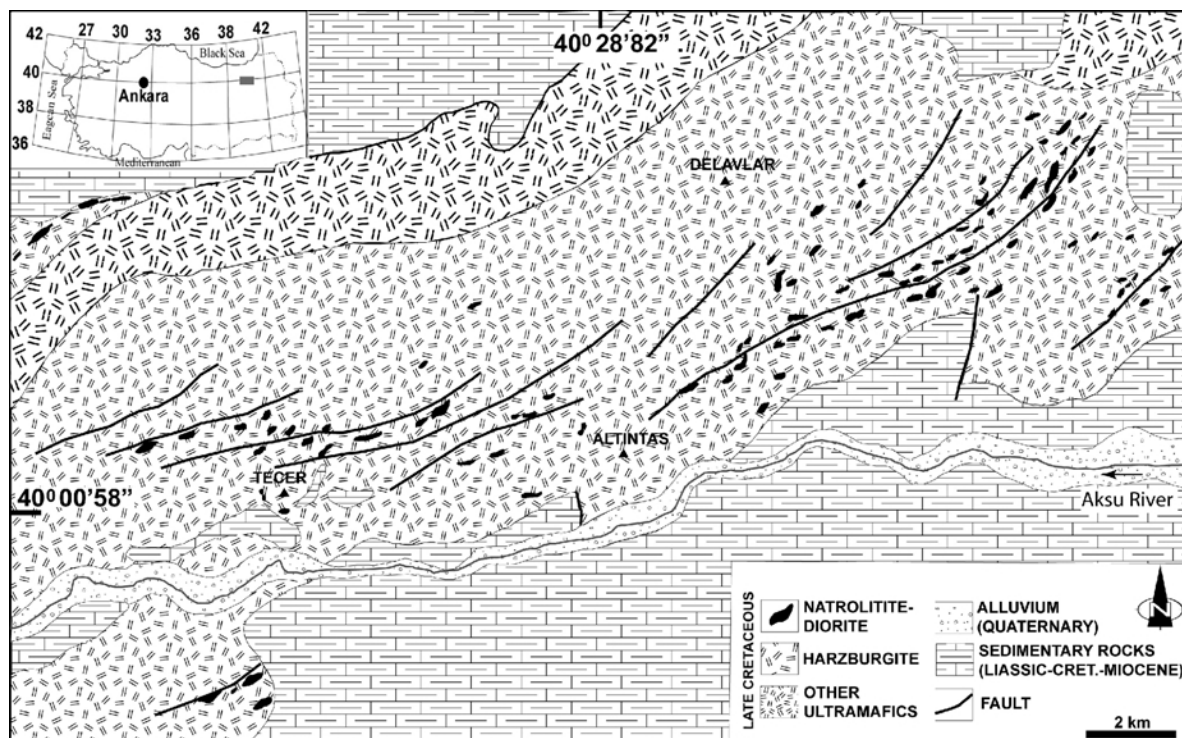
Figure 1. Geological map of the study area. Inset map shows location of the Kop mountains complex and the natrolitized dikes (natrolitites are not to scale).

purpose of this paper is to report on the geological setting and to describe the mineralogical, petrographical, and geochemical aspects of natrolitite and the metasomatic process of natrolitization that produced these unique rocks. We speculate that other examples of natrolitites may occur elsewhere but may also have been overlooked because of the unique replacement process that produced the natrolite at the expense of plagioclase.

GEOLOGICAL SETTING

The natrolitites and pargasite natrolitites crop out within the extensive Upper Cretaceous Kop mountains complex between the southern zone of the Eastern Pontides and the Anatolides in eastern Anatolia, Turkey (Figure 1). The Kop mountains complex consists of ultramafic, mafic, and felsic rocks. The ultramafic rocks have a 'continental' rather than 'ophiolitic' geochemical signature (Figure 2) and are composed essentially of, progressing upwards, dunite, harzburgite, lherzolite, wehrlite, and pyroxenite, all of which have been variably serpentinized. Co-existing mafic and intermediate rocks include amphibolite, gabbro, diorite, diabase, basalt, and trondhjemite. With the exception of the basalts, the mafic and intermediate rocks occur in association with amphibolites. The basalts are part of the Senonian volcano-sedimentary sequence which rests unconformably on the Kop mountains complex (Kolaylı, 1996).

MATERIALS AND METHODS

Thin sections and polished thin sections from representative hand specimens were prepared for examination by transmitted light microscopy (TrLM), scanning electron microscopy (SEM), and electron microprobe analysis (EMPA). The TrLM investigations were conducted at the mineralogy laboratory of Karadeniz Technical University (Trabzon, Turkey). The SEM work was performed at the material research laboratory of Erciyes University
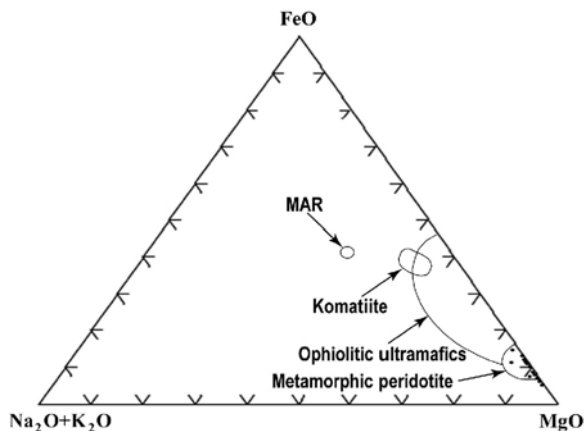

Figure 2. Ultramafic rock samples plot within the field of metamorphosed peridotites on the FeO_T-(Na_2O+K_2O)-MgO diagram of Coleman (1977).

(Kayseri, Turkey) using a computer-controlled LEO 440 system at 20 kV and 20 mA.

Forty eight rock samples representing the major rock types within this region were analyzed for major elements and a set of selected trace elements. Pressed-powder pellets 40 mm in diameter were prepared from ~6 g of sample mixed with a PVA binding agent, backed by ~5 g of boric acid powder under 400 kg/cm^2 of pressure for X-ray fluorescence (XRF) measurements (Schroeder *et al.*, 1980). X-ray fluorescence measurements were carried out at the Geological Engineering Department of Karadeniz Technical University, Trabzon, using a Jeol-SX2 X-ray fluorescence spectrometer (Table 1). The spectrometer was calibrated using USGS standards. Fourteen rock samples selected for *REE* analyses (by inductively coupled plasma-mass spectrometry − ICP-MS) and four samples, natrolitized to various degrees, were analyzed for major, trace, and rare earth elements at Acme Labs (Canada) (Tables 1, 2). Representative splits were powdered for X-ray diffraction (XRD). The XRD analyses were performed at the University of Missouri-Rolla, with a Scintag, Inc, XDS 2000, using Ni-filtered CuKα (λ = 1.5405 Å) as the radiation source in step-scan mode, with 0.01°2θ per step. X-ray powder diffraction patterns were evaluated using *Jade* software (Materials Data, Inc., Livermore, California).

The compositions of the natrolites, plagioclase, and pargasites were determined by wavelength dispersive X-ray analysis using a Cameca SX50 electron microprobe (Pasabahce Glass, Ltd., Research Laboratories,

Istanbul). An accelerating voltage of 15 kV was used. The beam current and counting time for major elements were 20 nA and 20 s, respectively. Trace elements were analyzed at a beam current of 100 nA and a counting time of 30 s. The accuracy of the EMP analyses was monitored using reference materials of similar composition (Tables 3, 4).

RESULTS

The Kop mountain complex

Ophiolitic, ultramafic rocks are common in eastern Anatolia (Bektas, 1981, 1982; Buket and Ataman, 1982; Bektas *et al.*, 1984; Musaoglu, 1987; Aslaner and Kolaylı, 1996; Kolaylı, 1996). However, the geochemical character of the ultramafic rocks from the Kop mountain complex exhibits a well defined continental affinity suggesting a distinctly different origin for these rocks. It should be noted that even though these rocks preserve igneous textures, their whole-rock geochemistry demonstrates the pervasive nature of Na metasomatism (Tables 1, 2). This metasomatic event has had different degrees of impact on these rocks such that the more immobile elements (*e.g.* Ti, Zr, heavy rare-earth elements) retained their relative primary abundances and can be used, with caution, to gain preliminary insight into the character and origin of these rocks. The ultramafic rocks plot within the field of metamorphosed peridotites on the FeO$_T$-(Na$_2$O+K$_2$O)-MgO diagram of Coleman (1977) (Figure 2). Their *REE* abundances correlate well with average values of continental
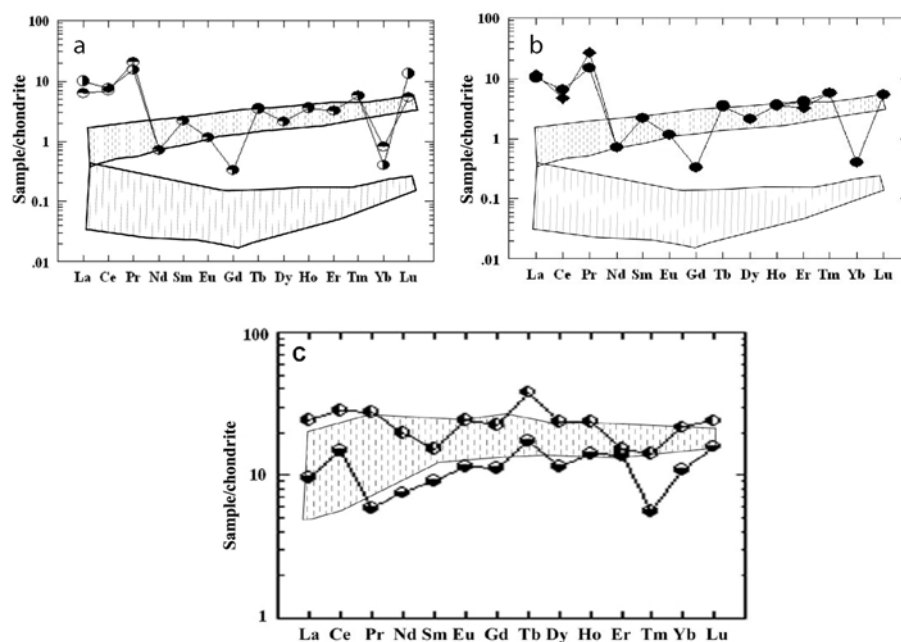

Figure 3. Chondrite-normalized *REE* data of the ultramafic rocks: (a) dunite; (b) harzburgite; and (c) amphibolite correlate well with average values of the continental ultramafic rocks (stippled pattern − continental ultramafic rocks; vertical striped pattern − ophiolitic ultramafic rocks) (Bodinier, 1988; Prinzhofer and Allegre, 1985; Schüssler *et al.*, 1989).

ultramafics (Figure 3a, 3b). The geochemical characteristics of the mafic and intermediate rocks of the Kop mountain complex are more diverse than the ultramafic rocks. Amphibolite occurs as lenses or stocks within the ultramafic rocks. They are geochemically similar to the basalts and diabase with regard to major and trace-element data (Table 1). The amphibolite *REE* abundances are similar to those of mid-ocean ridge basalt (MORB). Their chondrite-normalized *REE* data vary between 6 and 40 ppm, which coincides with the data of amphibolites associated with continental peridotites (Figure 3c). Rare gabbro crops out within the complex

as well. These rocks are remarkably depleted in TiO_2 and Rb and have *REE* abundances that coincide with ophiolitic gabbros. Diorite is much more common throughout the Kop mountain complex and is geochemically similar to the gabbro, but will be discussed later due to its close spatial association with the natrolitites. Diabase also occurs in association with the gabbro and diorite. The geochemical signature of the diabase is similar to those of gabbros and diorites (*e.g.* TiO_2 content) and they plot in the IAB field on the Ti-Zr diagram of Pearce (1982). As for the ultramafic rocks, the whole-rock geochemistry also demonstrates the

Table 1. Major-oxide (wt.%) and trace-element (ppm) contents of ultramafic, mafic, and intermediate rocks of the Kop mountains complex.

Sample	Dunite1	Dunite2	Dunite3	Dunite4	Dunite5	Dunite6	Dunite7	Harz1	Harz2	Harz3	Harz4	Harz5
SiO_2	42.8	45.57	42.76	42.78	46.43	42.45	42.77	44.48	45.36	45.16	45.62	46.02
TiO_2	0.03	0.02	0.03	0.03	0.01	n.d.	0.03	0.04	0.04	0.05	0.02	0.14
Al_2O_3	0.07	0.63	0.06	0.06	0.13	0.03	0.06	1.28	0.99	1.7	0.63	1.52
FeOT	4.26	8.46	4.32	4.23	6.14	7.12	4.33	7.75	11.55	8.08	8.49	11.27
MnO	0.07	0.14	0.05	0.08	0.09	0.15	0.07	0.12	0.17	0.13	0.14	0.13
MgO	52.55	44.41	52.56	52.65	47.02	50.08	52.59	44.61	35.15	42.41	44.29	40.06
CaO	0.19	0.69	0.21	0.11	0.02	0.14	0.11	1.36	6.57	2.39	0.69	0.75
Na_2O	n.d.	0.07	n.d.	0.05	0.05	0.05	0.02	0.03	0.09	0.08	0.11	0.09
K_2O	0.10	0.01	n.d.	0.01	0.05	0.01	n.d.	0.19	0.40	0.01	0.01	0.01
P_2O_5	n.d.	n.d.	n.d.	n.d.	0.06	n.d.	n.d.	0.08	0.05	n.d.	n.d.	n.d.
Ba	0.16	1.97	6.00	2.20	5.02	4.90	7.57	7.00	9.00	7.51	7.27	4.58
Rb	1.66	0.28	4.16	2.46	2.41	5.15	0.76	1.27	1.44	3.00	1.18	3.12
Sr	1.00	0.44	0.71	1.12	1.85	0.87	1.33	2.14	1.23	0.52	0.36	3.91
Y	n.d.	n.d.	0.10	0.08	0.20	n.d.	0.01	0.20	0.40	0.01	0.07	0.02
Zr	11.7	5.26	12.48	8.8	10	9.99	4.98	5.17	7.32	8.45	7.57	31.13
Nb	2.61	1.20	1.45	1.49	1.02	1.39	1.62	0.91	1.13	1.33	0.71	1.03
Th	0.05	0.02	0.02	0.09	0.34	0.02	0.11	0.20	0.21	0.17	0.22	0.03
Ni	2186	2180	2312	2386	2498	2002	2382	1844	799	2192	2382	2323
Cr	7280	2337	7686	7238	2540	4162	7739	3010	6490	3442	2354	2306
La	0.54	0.18	0.22	1.46	4.10	0.11	1.17	3.60	2.30	0.79	0.81	0.26
Ce	2.38	0.31	0.06	1.72	11.10	0.10	2.38	13.00	10.00	0.07	0.27	0.16

Sample	Harz6	Lher1	Lher2	P_Lher1	P_Lher2	Prxt1	Prxt2	Prxt3	Prxt4	Wher1	Wher2	Amph1
SiO_2	46.03	45.14	44.56	42.65	44.63	55.71	53.16	44.93	38.23	44.43	43.82	50.12
TiO_2	0.14	0.13	0.13	0.04	0.34	0.22	0.20	0.01	0.19	0.01	0.02	0.45
Al_2O_3	1.50	1.67	1.64	11.02	4.37	6.40	6.77	0.05	9.02	0.06	0.05	8.12
FeO_T	11.25	11.93	12.87	5.38	10.06	5.38	4.47	8.61	16.01	8.75	8.86	11.32
MnO	0.13	0.27	0.27	0.18	0.22	0.11	0.06	0.18	0.21	0.19	0.20	0.16
MgO	40.09	39.99	39.52	32.53	37.83	16.44	20.68	45.8	35.38	46.36	46.85	25.50
CaO	0.75	0.86	0.96	7.79	2.38	15.14	14.09	0.15	0.15	0.17	0.17	4.48
Na_2O	0.08	0.01	0.04	0.37	0.14	0.51	0.49	0.28	0.60	0.02	0.01	0.67
K_2O	0.01	0.01	0.01	0.02	0.01	0.03	0.03	0.01	0.08	n.d.	n.d.	0.11
P_2O_5	n.d.	0.01	0.01	0.01	n.d.	0.06	0.06	n.d.	0.06	n.d.	n.d.	0.06
Ba	5.57	8.56	2.97	3.87	2.61	34.92	22.57	3.80	233.7	3.88	12.02	200.80
Rb	2.07	1.31	2.66	1.05	0.48	8.23	21.51	14.68	87.30	1.80	0.39	3.51
Sr	3.62	2.85	2.51	74.68	6.87	82.87	100.98	0.58	146.74	0.23	0.06	135.39
Y	n.d.	0.02	n.d.	0.45	0.20	2.27	0.78	0.01	5.22	0.07	0.03	12.40
Zr	58.23	23.23	14.52	3.72	168.6	21.70	26.55	8.26	41.26	13.69	4.72	86.09
Nb	3.62	1.18	0.99	0.62	0.03	1.93	2.45	0.77	1.84	0.47	0.69	2.02
Th	1.12	0.11	0.02	0.85	0.68	10.39	16.10	0.11	39.4	0.08	0.08	0.66
Ni	2326	2330	2319	441	2009	197	299	2084	3227	2394	2383	1006
Cr	2335	1635	1606	544	1939	2405	4524	3544	7238	1981	1931	1631
La	0.10	0.04	0.22	8.51	0.93	0.02	1.01	0.01	3.73	0.20	0.98	9.33
Ce	2.71	3.45	0.27	1.98	6.06	114.72	125.11	3.37	188.29	0.02	0.19	37.99

pervasive nature of the Na metasomatism even though they still preserve igneous textures (see Tables 1, 2). Geochemical characterization of the igneous origin of these rocks must be viewed as preliminary until the extent of the effect of this metasomatic alteration is better constrained. The trondhjemite exhibits low TiO_2, extremely low MgO, high Na_2O, and remarkably high Rb contents (Table 1). They are calc-alkaline (Figure 4b) and plot within the volcanic-arc granite field on the Pearce *et al.* (1984) diagram, and are continental in character on the K_2O-SiO_2 diagram of Coleman (1977). The basaltic rocks are tholeiitic with trace element affinities to MORB and Within Plate Basalts (WPB) (Figure 4a, 4b).

The diorite-natrolitite complexes

The ultramafic rocks, largely harzburgites, of the Kop mountains, were intruded by diorite which was subsequently metasomatized to form the natrolitites. These intrusions occur as dikes and elongate stocks, ~5 m ×

Table 1 (*contd.*)

Sample	Amph2	Gabbro1	Gabbro2	Diorite1	Diorite2	Trondhj1	Trondhj2	Trondhj3	Trondhj4	Trondhj5	Trondhj6	Diabase1
SiO_2	42.94	45.16	46.65	56.29	49.42	76.09	77.57	77.74	74.00	74.38	74.49	68.75
TiO_2	1.93	0.23	0.23	0.25	2.01	0.11	0.15	0.15	0.15	0.18	0.16	0.57
Al_2O_3	11.79	25.57	19.44	10.58	10.98	11.97	12.69	12.8	13.26	13.01	13.56	13.7
FeO_T	21.49	4.07	0.01	5.52	17.18	2.86	2.33	2.17	1.59	2.26	3.87	5.08
MnO	0.30	0.05	4.89	0.09	0.25	0.05	0.02	0.02	0.02	0.03	0.06	0.10
MgO	8.80	7.95	0.07	13.31	6.51	3.82	0.57	0.18	0.32	0.45	0.91	0.97
CaO	7.74	14.16	10.56	12.51	10.73	0.06	0.33	1.11	2.48	2.11	0.86	0.78
Na_2O	4.22	1.75	16.60	1.28	2.46	4.30	5.86	5.34	4.90	4.49	5.16	9.74
K_2O	0.61	1.01	1.12	0.10	0.26	0.72	0.49	0.46	3.23	3.04	0.87	0.16
P_2O_5	0.17	0.05	0.28	0.06	0.21	0.03	0.02	0.02	0.04	0.05	0.05	0.15
Ba	127.21	98.25	117.72	78.49	68.38	100.51	92.00	182.00	126.78	69.27	178.5	197.87
Rb	11.27	1.01	3.50	7.71	8.80	20.18	23.20	19.30	19.60	18.24	24.94	10.26
Sr	39.96	376.1	159.03	251.76	107.10	31.12	64.00	76.00	27.20	181.90	46.40	67.66
Y	53.66	2.850	2.33	2.72	47.41	23.90	36.80	33.70	9.30	13.88	30.22	24.19
Zr	120.11	10.48	3.59	28.98	155.92	226.3	128.00	125.00	168.90	168.70	185.93	77.38
Nb	6.52	1.62	1.81	1.19	5.75	7.71	10.00	10.00	6.03	4.29	4.92	8.10
Th	3.80	3.36	2.08	0.78	1.97	0.43	0.76	0.83	7.06	10.85	0.24	5.99
Ni	29.00	46.00	135.00	66.00	23.00	16.00	14.00	14.00	16.00	17.00	13.00	7.00
Cr	5.00	404	348	87.00	26.00	22.00	18.00	22.00	5.00	5.00	16.00	2.00
La	9.11	2.70	2.69	2.88	8.56	6.52	8.20	10.10	16.85	9.65	5.46	7.92
Ce	9.54	74.64	92.00	81.67	13.80	15.18	32.00	48.00	28.68	31.67	15.66	33.25

Sample	Diabase2	Diabase3	Basalt1	Basalt2	Basalt3	Basalt4	Basalt5	Basalt6	Nat1	Nat2	Nat3	Nat4
SiO_2	68.95	76.65	55.88	47.45	45.97	55.61	57.38	48.11	46.3	46.52	46.19	46.08
TiO_2	0.56	0.54	1.09	1.90	1.84	1.75	1.95	1.66	0.16	0.37	0.51	0.51
Al_2O_3	13.68	9.44	11.75	11.93	11.76	11.57	14.59	11.93	24.18	19.41	19.49	19.53
FeO_T	5.09	6.89	18.65	23.27	25.21	14.35	10.37	22.36	1.03	2.53	2.99	3.02
MnO	0.10	0.08	0.31	0.97	1.02	0.39	0.50	0.63	0.02	0.04	0.03	0.03
MgO	0.96	2.78	5.50	5.64	5.94	5.30	3.25	7.51	0.63	3.64	4.24	4.23
CaO	0.77	0.53	4.26	4.48	4.05	5.98	5.29	3.48	2.95	2.78	2.56	2.55
Na_2O	9.58	2.80	2.25	3.97	3.81	4.82	6.40	2.41	14.39	12.35	11.82	11.82
K_2O	0.16	0.19	0.11	0.24	0.26	0.08	0.10	1.78	0.16	0.26	0.71	0.64
P_2O_5	0.15	0.09	0.20	0.15	0.14	0.15	0.17	0.14	0.01	0.09	0.19	0.16
Ba	229.60	150.74	137.27	177.81	167.05	167.40	99.00	1609	190.00	482.00	375.00	369.00
Rb	10.21	12.76	8.99	9.86	10.41	6.92	8.33	21.98	2.59	11.52	29.33	29.06
Sr	64.72	20.36	139.06	159.67	148.42	45.47	73.00	113.90	315.00	418.00	517.00	522.50
Y	24.76	7.12	32.97	102.27	107.30	60.47	45.30	79.42	3.60	4.70	5.20	5.10
Zr	73.03	60.18	38.37	129.76	131.77	102.60	88.00	123.60	80.80	74.10	53.60	53.10
Nb	9.27	1.07	4.60	10.50	10.96	6.10	10.00	7.30	3.75	4.30	2.75	2.35
Th	4.18	3.99	0.70	1.72	1.61	2.17	3.91	3.75	1.30	3.90	3.10	3.10
Ni	7.00	4.00	15.00	15.00	15.00	11.00	11.00	22.00	5.00	24.00	20.00	20.00
Cr	1.00	7.00	6.00	2.00	1.00	1.00	3.00	8.00	8.00	23.00	25.00	24.00
La	8.14	2.87	4.81	9.58	9.96	7.94	8.00	45.66	5.40	17.00	14.20	14.20
Ce	3.74	58.50	59.68	8.64	7.57	17.05	23.80	36.12	10.00	28.00	24.60	23.80

n.d. − not detected; Harz − harzburgite; Lher − lherzolite; P_Lher − plagioclase lherzolite; Prxt − pyroxenite; Wher − wherlite; Amph − amphibolite; Trondhj − trondhjemite; Nat − natrolitite

Table 2. *REE* contents (ppm) of ultramafic, mafic, and leucocratic rocks of the Kop mountains complex.

Sample	Dunite1	Dunite2	Harz1	Harz2	Prxnt1	Prxnt2	Diorite1	Diorite2	Amph1
Y	0.2	0.2	0.2	0.4	1.1	0.2	4.4	2.8	27.3
La	3.7	4.1	3.6	2.3	3.1	3.6	2.5	1.1	3.5
Ce	6.2	4.5	7.3	6.5	9.4	9.4	7.4	5.8	14.1
Pr	2	3.6	2.1	2.8	0.6	4.2	1.9	0.4	0.8
Nd	0.5	0.5	0.5	0.5	0.5	0.5	0.5	0.5	5.3
Sm	0.5	0.5	0.5	0.5	0.5	0.5	0.5	0.5	2.1
Eu	0.1	0.1	0.1	0.1	0.1	0.1	0.3	0.1	1
Gd	0.1	0.1	0.1	0.1	0.1	0.1	0.3	0.1	3.4
Tb	0.2	0.2	0.2	0.2	0.2	0.2	0.4	0.4	1
Dy	0.8	0.8	0.8	0.8	0.8	0.8	0.8	0.8	4.4
Ho	0.3	0.3	0.3	0.3	0.3	0.3	0.3	0.3	1.2
Er	1	0.8	0.8	0.8	0.8	0.8	1.3	1.3	3.4
Tm	0.2	0.2	0.2	0.2	0.2	0.2	0.2	0.2	0.2
Yb	0.1	0.1	0.1	0.2	0.2	0.1	0.7	0.7	2.7
Lu	0.2	0.2	0.5	0.2	0.2	0.3	0.4	0.4	0.6

Sample	Amph2	Basalt1	Basalt2	Diabase1	Diabase2	Nat1	Nat2	Nat3	Nat4
Y	52.4	45.3	52.4	8.1	7.4	3.6	4.7	5.2	5.1
La	8.9	8	11.4	1.6	1.1	5.4	17	14.2	14.2
Ce	27	23.8	25.6	8.1	7.1	10	28	24.6	23.8
Pr	3.8	4.6	7.1	1.5	0.3	1.17	2.96	2.67	2.7
Nd	13.8	9.8	8.8	1.3	0.4	4.4	10	9.8	9.6
Sm	3.5	3	5.4	0.5	0.5	1.4	1.9	2.1	2.1
Eu	2.1	1.7	2.2	0.3	0.1	0.47	0.54	0.68	0.6
Gd	6.8	6.5	5.8	0.7	0.4	1.36	1.97	2.02	2.07
Tb	2.2	1.9	1.7	0.4	0.4	0.16	0.22	0.24	0.25
Dy	8.9	7.5	8.4	1.4	1.2	0.91	1.09	1.26	1.15
Ho	2	1.8	1.6	0.4	0.3	0.11	0.15	0.19	0.17
Er	3.8	4.5	4.9	1.4	1.2	0.35	0.49	0.5	0.61
Tm	0.5	0.5	0.6	0.2	0.2	0.04	0.06	0.06	0.06

10 m to 50 m × 150 m across, of quartz diorite transitional to microdiorite (Figure 8a). The long axes of these intrusions are oriented sub-parallel along a strike of N70ºE which coincides with the regional strike of the major oblique-slip reverse faults (Figure 1). The diorite intrusions appear to have exploited, and may even have sealed, these faults as they are undeformed with respect to these regional faults. Although the diorite intrusions have undergone extensive Na metasomatism to form the natrolitites, the larger stocks and dikes (typically >30 m × 50 m) preserve their original magmatic textures even though all the plagioclase has been albitized. In contrast, diorite intrusions smaller than ~30 m × 50 m have been converted completely to natrolitite. The significance of this size dependency is discussed later (see Figure 9). All natrolitized diorite
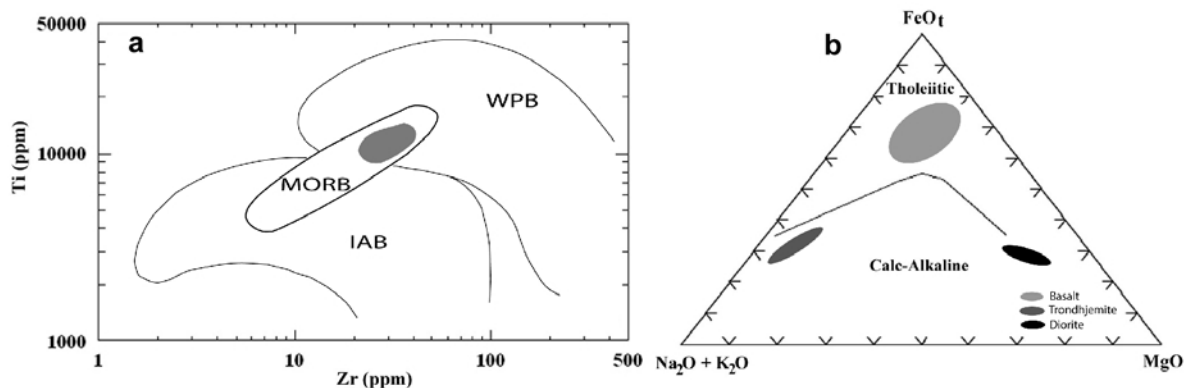

Figure 4. (a) Basaltic rock compositions (shaded field) plot in the MORB and the WPB fields on the Ti-Zr diagram of Pearce *et al.* (1984); (b) basalts plot within the tholeiitic basalt field, whereas trondhjemites and diorites plot in the calc-alkaline field on the (Na_2O+K_2O)-FeO_t-MgO triangle diagram of Irvine and Baragar (1971).

bodies are fractured and contained cm−mm-scale quartz veins (Figure 8a, 8b).

The major and trace-element data of diorite (Tables 1, 2) indicate that their TiO_2 and Rb contents are notably small. They plot within the calc-alkaline field on the $(Na_2O+K_2O)-FeO_t-MgO$ triangle diagram of Irvine and Baragar (1971). Chondrite-normalized *REE* values vary between 0.3 and 15 ppm. These values coincide with those of such rocks associated with ophiolites (0.6−10 ppm) (Figures 4b, 5). However, the pattern shown by the 'diorites' is much more irregular than those normally obtained from rocks of this type in other ophiolite complexes (Figure 3c). This could be due to the fluids causing the metasomatism. This is more noticeable when the chondrite-normalized *REE* data from the diorites were compared with those of the natrolitites (Figure 5). Thus, immobile elements were expected to retain their relative primary abundances to gain preliminary insight into the character and origin of these rocks.

The natrolitite and pargasite natrolitite crop out in a broadly NE−SW striking linear belt which coincides with the *en-echelon* fault system and the belt of diorite intrusions north of Aksu River (Figure 1). They are overlain by late Cretaceous sedimentary rocks consisting of sandstones and conglomerates in the south, and disconformably by Miocene sedimentary rocks in the north. Clasts of diorite are observed in the late Cretaceous conglomerates, but not in the early Cretaceous sedimentary rocks. Clasts of natrolitized diorite have yet to be found within either the early- or late-Cretaceous conglomerates. Thus, the unroofing of
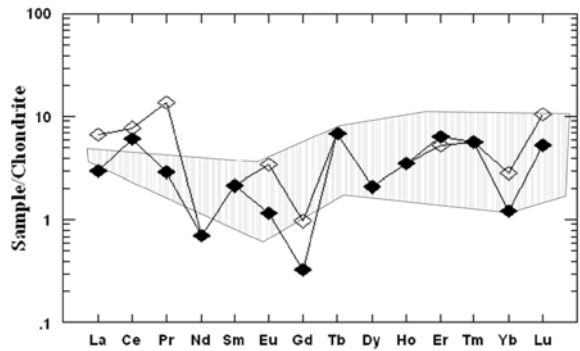

Figure 5. The *REE* data from diorites coincide with the average values of diorites associated with ophiolites (vertical striped pattern − ophiolitic ultramafics) (Coleman, 1977).

the diorite intrusions must be post-early Cretaceous and pre-late Cretaceous in age. While this field evidence (albeit negative evidence) appears to suggest a later (post Cretaceous) age for the Na-metasomatic event, we argue for the metasomatism to be associated with hydrothermal convection cells, set up by intrusion of the diorites themselves.

Smaller stocks and dikes ($\sim$<50 m $\times$ 150 m) of diorite within the ultramafic rocks ideally exhibit five zones, each characterized by a distinct mineral assemblage, as a result of this metasomatic event (Figure 6):

Central Zone 1. Diorite with magmatic textures preserved; alteration is limited to varying albitization; albite ± andesine ± pargasite ± quartz ± trace natrolite.
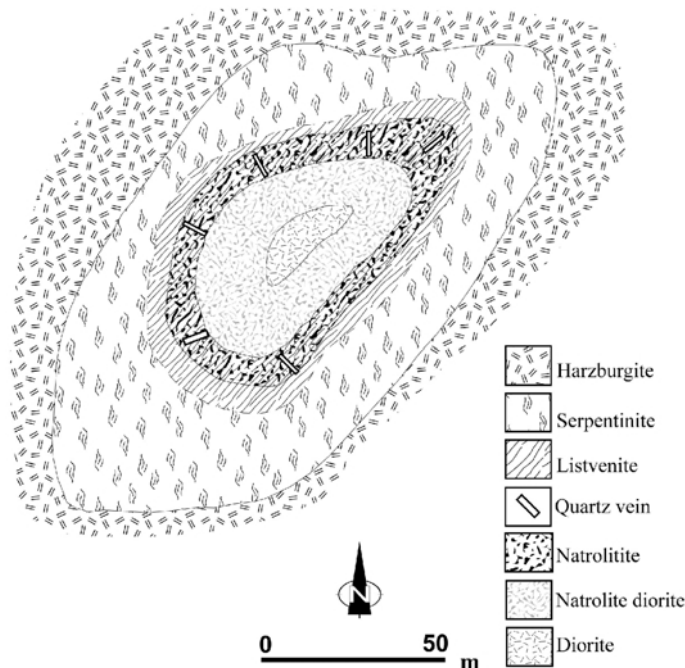

Figure 6. Concentric alteration haloes around the dikes of diorite intrusions.

Transition Zone 2. Natrolite-bearing diorite; relict magmatic textures are present; albite ± andesine ± natrolite ± pargasite ± calcite ± quartz.

Marginal Zone 3. Natrolitite and pargasite natrolitite cross cut by quartz-veins; consist of natrolite ± pargasite ± calcite ± chlorite ± trace albite.

Listvenite Zone 4. Magnesite ± quartz ± calcite ± mica ± hematite ± talc.

Brecciated serpentinite Zone 5. Hydrothermally altered and brecciated serpentinites.

The presence of these concentric zones depends on the size of the intrusion and intensity of the Na metasomatism. For the smaller intrusion (<50 m × 150 m), Zones 1 and 2 are variably preserved, and commonly, smaller diorite intrusions consist entirely of Zone 3 mineral assemblages. In contrast, the larger diorite stocks (>50 m × × 150 m) are typically only albitized (Zone 1) although natrolite tends to be present in minor to trace quantities. The natrolitite and pargasite natrolitites (Zone 3) are cross cut by quartz veins (Figures 6, 8b). Zone 3 is surrounded by listvenite − a unique rock in its own right. The listvenites consist of magnesite, quartz, calcite, mica, talc, and hematite. The listvenite zone can reach up to 20 m in size. Enveloping the listvenites is Zone 5, a poorly defined elliptical zone of brecciated serpentinite. The shatter-zone of brecciated serpentinite can be up to 200 m wide. Even though the region is still tectonically active, field observations suggest that brecciation of serpentinites is related to either the initial faulting, or to emplacement of these intrusions rather than post-dike emplacement tectonism.

Zonal petrographic and geochemical characteristics of the natrolitite complexes

Zone 1. Detailed petrographic studies revealed that primary magmatic textures were preserved in the central part (Zone 1). Prevalent textures are doleritic (subophitic) and/or interstitial. Modal analyses of the core rocks (Zone 1) indicate that equigranular diorites contain plagioclase (up to 95% of the phenocrysts) and pargasitic amphibole (up to 10%). Orthoclase and quartz are always present in trace amounts. The porphyritic diorites are composed of up to 35 vol.% plagioclase phenocrysts set in a microcrystalline groundmass of plagioclase and hornblende. Plagioclase crystals of Zone 1 in diorite are typically andesine with An_{41-38} and they are partly albitized (Table 3). Pargasitic amphibole occurs in rocks of all three zones. They typically appear as needles or prisms under TrLM and SEM. The TrLM examinations showed that pargasites with positive elongation have $2V_Z$ angles ranging between 40 and 50º. The composition of pargasite systematically increases in Na_2O content and decreases in CaO content outwards from Zone 1 to Zone 3 (Table 4). The average contents of Na, Ca, Mg, and K in the analyzed crystals are 1.08, 1.78, 3.37, and 0.06, respectively.

Table 3. EMPA data of plagioclases in parent rocks (1−3), in the natrolite-bearing zone 2 rocks (4−6), of natrolite in natrolite-bearing zone 2 rocks (7−12) and of natrolite in natrolitite (zone 3) (12−17) (each analysis represents the average of three analyses). The table also includes normative Ab-An-Or contents of plagioclases.

	1	2	3	4	5	6	7	8	9	10	11	12	13	14	15	16	17
SiO_2	57.14	56.82	58.87	57.59	65.21	63.10	48.68	48.43	47.08	47.81	46.48	48.08	47.68	48.43	46.46	47.81	48.41
Al_2O_3	27.10	27.71	27.70	26.46	22.63	24.73	26.32	25.74	26.41	26.21	27.20	27.55	26.32	25.90	25.41	25.21	26.20
TiO_2	n.d.	n.d.	n.d.	0.31	0.24	n.d.	n.d.	0.40	n.d.	n.d.	n.d.	0.33	n.d.	0.43	n.d.	n.d.	n.d.
FeO_T	0.31	n.d.	n.d.	0.16	0.32	0.43	n.d.	n.d.	n.d.	0.14	0.30	0.36	n.d.	n.d.	n.d.	0.12	0.29
CaO	8.19	7.93	7.42	7.00	1.36	2.04	0.11	1.20	1.09	0.12	0.51	n.d.	0.17	0.90	0.59	0.42	0.75
Na_2O	7.12	7.34	5.88	8.05	10.05	8.34	14.42	15.12	14.22	15.21	14.39	15.11	14.42	15.12	15.22	14.21	14.33
K_2O	0.14	0.08	0.12	n.d.	0.19	1.20	n.d.	0.16	n.d.	0.24	0.31	0.06	n.d.	0.19	n.d.	0.22	0.33
Total	100.00	99.88	99.99	99.57	100.00	99.84	89.53	91.01	88.80	89.73	89.19	91.49	88.59	90.78	87.68	87.99	90.31

Atomic proportion on the basis of 32 atoms

	1	2	3	4	5	6	7	8	9	10	11	12	13	14	15	16	17
Si	10.26	10.20	10.20	10.44	11.44	11.14	11.09	10.97	10.87	9.74	9.53	9.59	9.77	9.75	9.70	9.89	9.79
Al	5.74	5.86	5.86	5.79	4.68	5.14	7.07	6.87	7.19	6.29	6.57	6.48	6.36	6.15	6.25	6.14	6.24
Ti	0	0	0	0	0.03	0	0	0.06	0	0	0	0.05	0	0.06	0	0	0
Fe^{3+}	0.05	0	0	0	0.05	0.06	0	0	0	0	0.05	0.06	0	0	0	0.09	0.05
Ca	1.58	1.52	1.52	1.41	0.26	0.39	0.03	0.29	0.27	0.02	0.11	0	0.04	0.19	0.13	0.02	0.16
Na	2.48	2.55	2.55	2.02	3.42	2.85	6.37	6.64	6.37	6.01	5.72	5.85	5.73	5.90	6.16	5.70	5.62
K	0.03	0.02	0.02	0.02	0.04	0.27	0	0.03	0	0.06	0.08	0.02	0	0	0	0.06	0.08
An	39	38	41	32	7	11											
Ab	61	62	58	68	92	81											
Or	1	0	1	0	1	8											
Si/Al							1.57	1.60	1.51	1.55	1.45	1.48	1.54	1.58	1.55	1.61	1.57

n.d.: not determined

Table 4. EMPA data of pargasitic amphiboles in parent rocks (zone 1), in the natrolite-bearing zone 2 rocks and in natrolititic zone (zone 3).

	Zone 1	Zone 2		Zone 3	
SiO_2	44.02	45.52	45.98	44.13	44.74
TiO_2	1.66	1.54	1.84	1.98	1.69
Al_2O_3	14.49	13.20	13.09	14.50	13.10
FeO	11.49	8.63	8.11	10.90	7.86
MgO	13.59	15.96	16.22	13.62	17.29
CaO	11.36	11.60	11.46	11.09	11.00
Na_2O	3.04	3.14	2.56	3.17	4.09
K_2O	0.35	0.28	0.27	0.44	0.24
Total	100.00	99.87	99.53	99.83	100.01
Si	6.54	6.68	6.73	6.55	6.57
Ti	0.18	0.17	0.20	0.22	0.18
Al	2.54	2.86	2.26	2.54	2.26
Fe	1.43	1.06	0.99	1.35	0.96
Mg	3.01	3.49	3.54	3.01	3.78
Ca	1.81	1.82	1.80	1.76	1.73
Na	0.87	0.89	0.72	0.91	1.65
K	0.06	0.05	0.05	0.08	0.08

Zone 2. Rocks within the transition zone exhibit similar textures to rocks from Zone 1 (the core) with the addition of sparse to abundant crystals of natrolite. Modal analysis of these rocks indicates that they are composed of plagioclase (10 vol.%;), pargasitic amphibole (5−15 vol.%), and natrolite (5−80 vol.%). Within Zone 2 (and Zone 3), pargasitic amphibole is variably chloritized (γ:Z

= 20−26º; bluish green in the *X* direction, yellowish green in the *Z* direction; $2V_Z$ = 50−55º). Plagioclase crystals are either partially or completely replaced by natrolite crystals (Figure 8c). Natrolite pseudomorphs after plagioclase are common. Plagioclase from Zone 2 natrolite-bearing diorites are typically An_{32-37} and exhibit a lower and broader range in anorthite content than plagioclase from Zone 1. Albitization of plagioclase is also more common and more complete within Zone 2 (Figure 7a). Calcite and chlorite are commonly present as alteration products of pargasitic hornblende. Calcite also occurs filling intergranular spaces and along the grain boundaries of natrolite crystals.

Zone 3. Rocks of Zone 3 consist mainly of natrolite. The XRD and modal analysis indicate that they contain natrolite (up to 95 vol.%), calcite, pargasite, and chlorite after pargasite (all accounting for a total of <5 vol.%). Pargasite crystals occur as needles, radiating mats of needles, or prisms with needle fringes, and can appear fibrous. Plagioclases are completely replaced by natrolite and natrolite typically occurs as laths and grains with irregular outlines. Observation by SEM shows natrolite occurring in the same prismatic forms rather than in acicular or radiating crystals that are typical of natrolite (Figure 8c−f). Thus, natrolite pseudomorphs after plagioclase are very common in the metasomatized diorites. Albite was not observed. The natrolite grains are compositionally homogeneous (Table 3; Figure 7b, 7c). They exhibit a narrow range of Si/Al ratios (1.45 to 1.61)
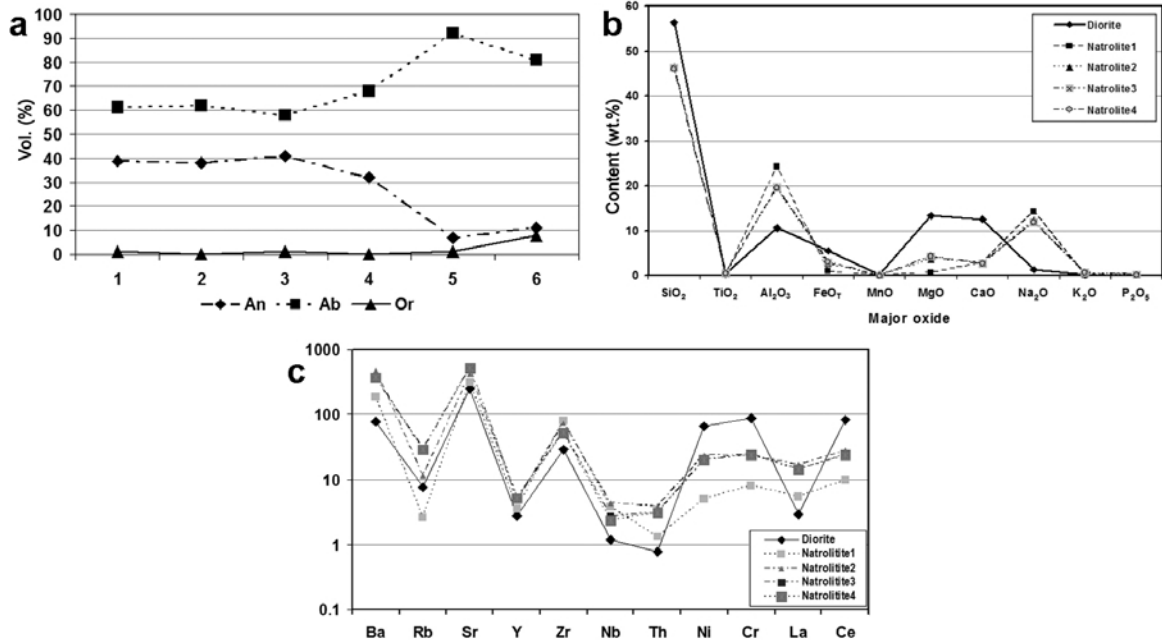

Figure 7. (a) Major chemical changes in the mineral composition (Ab-An) based on the EMPA data outwards from the center; (b) changes in bulk composition based on whole-rock data; (c) changes in bulk composition based on the whole-rock data for common trace elements.
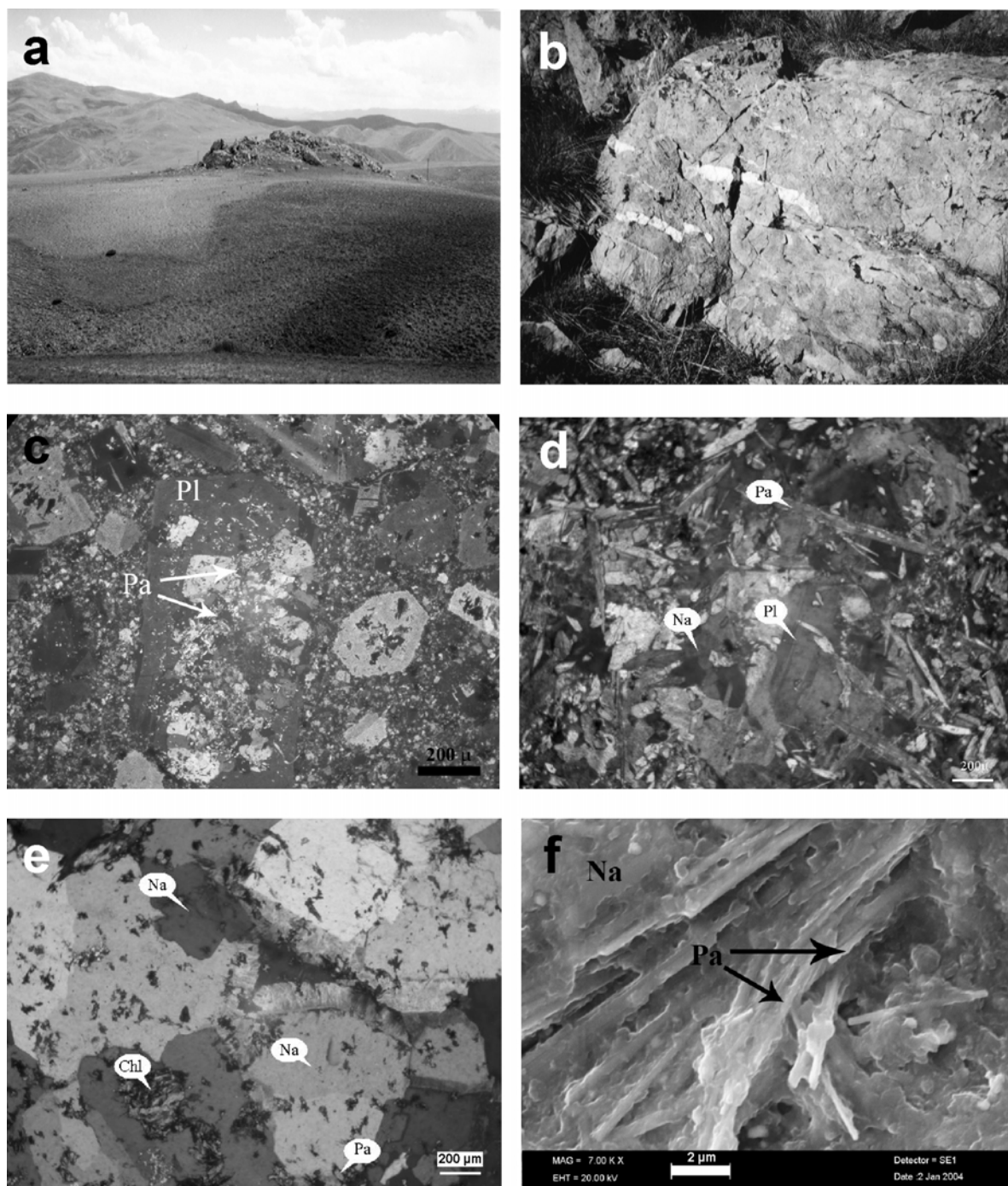
Figure 8. (a) Field view of natrolititic dike cropping out as elevated terrain (the adjacent electricity poles, 9 m tall, give scale); (b) m-scale natrolitite block with cm-scale quartz veins; (c) natrolite-bearing diorite; (d) pargasite natrolitite; (e) natrolite pseudomorphs after primary igneous plagioclase with trace pargasite and chlorite in natrolitite; (f) pargasite needles within natrolitic ground (Pa: pargasite, Na: natrolite, Chl: chlorite, Pl: plagioclase).

which is very similar to the Si/Al ratios of other natrolites (Ibrahim, 2004; Ross *et al.*, 1992; Hay, 1980). The average Na, Ca, and K contents are 6.06, 0.11, and 0.03, respectively. Fe^{3+} and Ti are present in trace amounts and Mg concentrations were below

detection limits. Calcite is typically present filling intergranular spaces.

Zone 4. Rocks of Zone 4 are composed of listvenite, a silicified serpentinite. It envelopes Zone 3, the natroli-

titic zone, in a roughly elliptical zone extending up to 20 m in thickness. Macroscopically the listvenite occurs in shades of brown, due essentially to the high hematite content, and is extremely hard and rigid as a result of intense silicification. This intense alteration has obliterated all original textures. Petrographic and XRD studies were used to characterize the mineral assemblage of the Listvenite Zone, which consists of magnesite, quartz, calcite, mica, hematite, and talc.

Zone 5. Zone 5 consists of brecciated serpentinites. It surrounds the whole structure and may reach up to 200 m thick. The brecciated serpentinites are various shades of green in color. Clast sizes vary greatly from cm-scale to m-scale. The breccias contain abundant late hydrothermal calcite and quartz veins that formed after and possibly during brecciation. The brecciation is considered to be coeval with emplacement of the diorite intrusions.

DISCUSSION

Natrolite is the most common of the zeolite species of the natrolite group. Although it can originate from alteration of a variety of starting materials, volcanic glass is the usual precursor. The formation of natrolite, as is the case for many of the zeolite minerals, is very dependent on the activities of dissolved species in the fluid phase including alkali and alkaline earth ions (*e.g.* Na, K, Ca), H_4SiO_4, and $Al(OH)_4^-$. Under high pH conditions (>9), mainly saline and very alkaline environments, the formation of zeolites is favored over the clay minerals. The solubility of SiO_2 and Al species also increases at high pH values (Hay and Sheppard, 2001).

Conversion of the primary igneous mineral assemblage of the diorites (Zone 1) to that of the natrolitite and pargasite natrolitite (Zone 3) can be viewed in the system $CaO-Na_2O-K_2O-Al_2O_3-SiO_2$ and a Na-rich, Si-rich fluid phase containing variable amounts of CO_2. Within this system, natrolite and albite, as well as the minerals mordenite, analcime, and paragonite can be expected to form, based on stability and activity diagrams (Chipera and Apps, 2001; Birsoy, 2002). What makes the natrolitite and pargasite natrolitites of the Kop mountain complex so unusual is that these rocks consist entirely of natrolite and albite, whereas the other secondary alteration minerals (zeolites, particularly paragonite) were not detected. In addition, the formation of these rock types appears to be the result of a metasomatic replacement of plagioclase by natrolite rather than direct precipitation of zeolite minerals from a fluid phase.

The abundance of natrolite pseudomorphs after plagioclase in these rocks is consistent with the formation of natrolite as a result of metasomatic replacement of plagioclase. Theoretically, this could

have occurred in a one-step process by conversion of plagioclase to natrolite as a result of Na-Si metasomatism. This would require simultaneous hydration and silicification of the plagioclase and replacement of Ca by Na through a reaction such as:

$$CaAl_2Si_2O_8 + Na_{(aq)}^+ + H_4SiO_4 \rightarrow$$
$$Na_2Al_2Si_3O_{10} \cdot 2H_2O + Ca^{2+} \qquad (1)$$
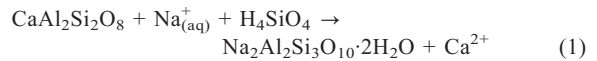
Although formation of natrolite by this process cannot be ruled out in all instances, several observations argue in favor of a two-step process of replacement of plagioclase to form natrolite instead. Within the diorite-natrolitite complexes, plagioclase crystals show a systematic decrease in An contents and an increase in Ab contents from Zone 1 out to Zone 3 as natrolite becomes increasingly more prevalent (Table 3). In addition, although plagioclase crystals in Zone 1 still preserve their igneous textures they also record the initial stages of albitization, such that by Zone 2 the composition of the remaining plagioclase crystals (those which were not converted to natrolite) is that of albite (Figure 7a). By Zone 3 the plagioclase crystals have been converted completely to natrolite, but they still retain the original primary igneous textures (Figure 8e).

Initially, albitization may have taken place through deuteric reactions at relatively higher temperatures along a reaction of the form:

$$CaAl_2Si_2O_8 + 2Na_{(aq)}^+ + 4H_4SiO_4 \rightarrow$$
$$2NaAlSi_3O_8 + Ca_{(aq)}^{2+} + 8H_2O \qquad (2)$$
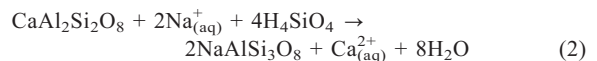
This reaction predicts a large ΔV_{solids} for this reaction as a result of the formation of two moles of albite from one mole of anorthite. In contrast, preservation of the primary igneous plagioclase textures is more consistent with a one-for-one replacement process of the anorthitic component of plagioclase by albite and then albite by natrolite. Thus, conversion of the primary igneous plagioclase to albite is more likely to have taken place through the following reaction:

$$CaAl_2Si_2O_8 + Na_{(aq)}^+ + H_4SiO_{4\ (aq)} \rightarrow$$
$$NaAlSi_3O_8 + Ca_{(aq)}^{2+} + Al(OH)_{4\ (aq)}^- \qquad (3)$$
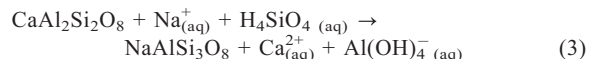
The small decrease in molar volume from anorthite (~105 cm^3/mol) to albite (~103 cm^3/mol) would allow for preservation of the original igneous textures. Subsequent conversion of the albite to natrolite may have taken place *via* a reaction of the form:

$$NaAlSi_3O_8 + Na_{(aq)}^+ + Al(OH)_{4\ (aq)}^- \rightarrow$$
$$Na_2Al_2Si_3O_{10} \cdot 2H_2O + 1/2O_2 \qquad (4)$$
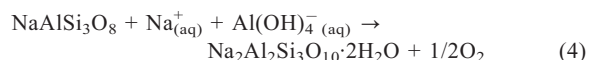
The Kop mountain natrolitites are unusual for two reasons: (1) the presence of natrolite and albite; and (2) the conspicuous absence of the more common alteration minerals, including paragonite, analcime, and calcic zeolites. The conversion of albite to paragonite (which was not observed as part of the metasomatic assemblage) would have taken place along a reaction of the following type:

$$NaAlSi_3O_8 + 2Al(OH)_4^-{}_{(aq)} \rightarrow$$
$$NaAl_3Si_3O_{10}(OH)_2 + 1/2O_2 \quad (5)$$
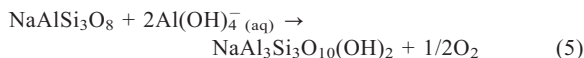
The stoichiometry of this reaction indicates that a smaller chemical potential of Na^+ and a greater chemical potential for Al^{3+} are required for paragonite to form as a result of the metasomatic alteration. In the case of the Kop mountain natrolitites, the source of Na and Si is presumed to have been derived externally from the fluid phase. In contrast, we suggest that the source of Al required for reaction 4 to take place originated internally from replacement of the anorthite component of the primary igneous plagioclase through progress along reaction 3 and therefore was limited in abundance. The absence of paragonite, which is typically the more common alteration mineral, and the presence of natrolite, in rock-forming abundance, instead reflects the large chemical potential of Na and the small chemical potential of Al during metasomatism. In addition, we suggest that the greater solubility of $Al(OH)_4^-$ in alkaline hydrothermal fluids would allow for transport of $Al(OH)_4^-$ derived from albitization of the primary plagioclase crystal, along with the Na^+ and H_4SiO_4, up towards the outer margins of the diorite intrusions (*i.e.* Zones 2 and 3). This resulted in a local increase in the chemical potential of Al to the point where natrolite replaced the albitized plagioclase to form the natrolitites *via* reaction 4 but not high enough to form paragonite *via* reaction 5 (Figure 9).

The absence of analcime ($NaAlSi_2O_6 \cdot H_2O$) reflects a greater chemical potential of SiO_2 at the time of metasomatism, consistent with the common occurrence of quartz veins in Zone 3 (Figure 8b). In addition, we suggest that the absence of calcic zeolites, especially with the release of Ca^{2+} ions into solution as a result of the albitization of plagioclase, reflects the presence of an additional component in the fluid phase, *i.e.* CO_2. The chemical activity of CO_2 is significant with regard to the activity of H_2O and the formation of calcite (Hay, 1966). High levels of CO_2 can significantly reduce the activity of H_2O as well as provide carbonate ions for the formation of calcite. Calcite is present as a minor phase in metasomatic Zones 2, 3, and 4. Thus the Ca^{2+} released during the albitization of the primary plagioclase (reaction 3) reacted with the $HCO_3^-{}_{(aq)}$ to form intergranular calcite. This suggests that the Na/Ca ratio of the system was always high enough to suppress the formation of calcic zeolites in favor of the formation of natrolite.

Hydrothermal circulation of Na-rich brine induced by the diorite intrusions can explain the formation of the natrolitite and pargasitic natrolitite. Albite formation in hydrothermally altered Icelandic basalts was observed above temperatures of 150ºC which is the lowest temperature for albitization (Apps, 1983). In contrast, most zeolites, with the exception of a few (*e.g.* analcime and wairakite), form at temperatures of <250ºC (Chipera and Apps, 2001). Experimental studies indicate that
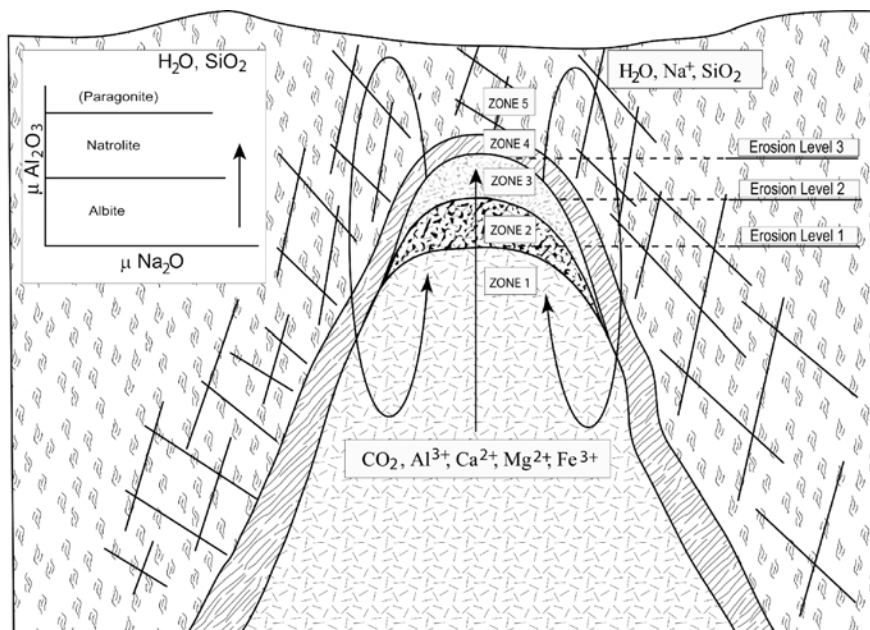

Figure 9. Schematic idealized cross-section of diorite intrusion into serpentinized country rocks. Hydrothermal circulation of Na-rich fluids (shown by arrows) scavenges elements, particularly Al and Ca, from primary plagioclase during albitization. These elements are transported by these fluids to higher levels in the intrusion to form natrolite. Concentric zonation and the extent of alteration for intrusions of different size are shown to be a function of the structural level exposed by erosion (for rock symbols, please refer to Figure 6).

stability fields for phillipsite, chabazite, erionite, and stilbite are completely eliminated at temperatures above 100ºC with higher temperatures favoring the formation of natrolite, thomsonite, and scolecite (Chipera and Apps, 2001). We suggest that albitization occurred first as the intrusions initially cooled and set up the hydrothermal circulation of fluids enriched in Na^+ and silica (*e.g.* H_4SiO_4) along reaction 3. A possible source for Na^+ could be leaching of the surrounding trondhjemites as they are significantly enriched in Na^+ (Table 1), which is more susceptible to leaching than the other alkaline earth elements (Ibrahim, 1996). Alternatively, the source of this fluid may have been Na^+-rich basinal brines that may have been present within the Kop mountain complex.

Hydrothermal circulation cells set up by the cooling diorite intrusion promoted mixing between the Na^+-rich fluid with a silica-rich and CO_2-rich (?) late-stage magmatic fluid originating from the final stages of crystallization of the diorites. Movement of this mixed fluid through the diorite albitized the primary igneous plagioclase *via* reaction 3. This reaction released Al^{3+} which was incorporated into the Na-rich alkaline fluid and transported a relatively short distance (see below) where it replaced already albitized plagioclase grains to form natrolite *via* reaction 4. Ca^{2+} ions released from igneous plagioclase during this alteration combined with CO_3^{2-} to produce intergranular calcite.

The zonal arrangement of the metasomatic zones and the correlation between their extent of development and the size of the diorite intrusions is consistent with an external source of a Na-rich fluid and a local and limited source of Al^{3+} (Figure 9). We suggest that the hydrothermal convection cells transported the Al^{3+} up towards the tops of the diorite intrusions. The smaller intrusions which are completely converted to natrolitite and pargasitic natrolitite represent structural levels where just the top of the intrusion has been exposed, and the source of the Al^{3+} was scavenged from deeper levels of the intrusion. Diorite intrusions exposed at slightly deeper structural levels reveal the concentric patterns of the metasomatic zones, and the largest intrusions, in which only Zone 1 (*i.e.* albitized diorite) or unaltered diorite is present, represent the deepest level of exposure and the source of the Al^{3+} needed to drive reaction 4 and form natrolite in the higher structural levels of the intrusions.

The final metasomatic zone (Zone 4) consists of a thin zone of listvenite which envelops the natrolitite zone (Zone 3) and is in turn surrounded by a fractured serpentinite zone (Zone 5) (see Figure 6). The hydrothermal circulation of the Na-rich, Si-rich, and CO_2-rich metasomatizing fluids through the diorite also scavenged Ca^{2+}, Mg^{2+}, Fe^{2+}, and Fe^{3+} as well as O_2 (see reaction 4) from the diorite protolith during its conversion to natrolitite and pargasitic natrolitite. This fluid exited the diorite and reacted with the serpentinite and/or

precipitated calcite ($CaCO_3$), magnesite ($MgCO_3$), and hematite (Fe_2O_3) (as a result of the oxidizing conditions) to form the thin zone of listvenite along the contact between the diorite and the brecciated serpentinite. Magnesite and talc in the listvenite zone can also be produced by reaction of serpentine with the CO_2 in the fluid phase via the following reaction:

$$2Mg_3Si_2O_5(OH)_4 + 3CO_2 = $$
$$Mg_3Si_4O_{10}(OH)_2 + 3MgCO_3 + H_2O \qquad (6)$$
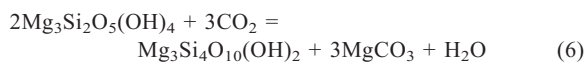
The fracturing and brecciation of the serpentinites is thought to be associated with intrusion of the diorites. Some brittle deformation (*e.g.* the fractures filled by quartz in the natrolitite zone) may reflect volume changes associated with the metasomatic process. However, since the diorites are intruded along a fault zone, and the area remains tectonically active, the possibility remains that the deformation could also have been the result of post-metasomatic tectonism.

CONCLUSIONS

A very unusual rock consisting of natrolite, with or without subordinate pargasite (<5 vol. %) and rare albite (<1 vol. %), has been discovered in the Kop mountain range in eastern Turkey. We propose that these rocks be called 'natrolitite' and those containing additional pargasite are termed 'pargasite natrolitite'. These natrolitites formed as a result of Na-metasomatic hydrothermal alteration of fault-controlled intrusions of igneous rocks with intermediate composition that crop out as dikes and stocks within a terrain consisting chiefly of serpentinized harzburgites. The natrolitization occurred through two-step replacement of primary igneous plagioclase, the first reaction resulted in albitization of the plagioclase, the Al released from the primary plagioclase was mobilized by the alkaline and CO_2-rich fluid and concentrated near the tops of these intrusions. This local increase in the chemical potential of Al enabled conversion of albitized plagioclase to natrolite by the metasomatic fluids. A zone of listvenite was formed along the contact between the diorite and the surrounding serpentinite as this fluid exited the intrusions. The result of this hydrothermal metasomatic alteration was the creation of concentric elliptical alteration zones centered around the original intrusions reflecting the structure level of exposure. Since the natrolite formed as a result of metasomatic replacement rather than precipitation from a fluid phase, the primary igneous textures of the plagioclase crystals were preserved in thin section, and the extent of the natrolitization of these rocks remained undetected at first. Although we believe this is the first report of such unusual rocks in the literature, we speculate that other examples of natrolitites may occur elsewhere and may also have been overlooked because of the nature of this unique replacement process that produced these rocks.

REFERENCES

Apps, J.A. (1983) Hydrothermal evolution of repository groundwaters in basalt. Pp. 14–51 in: *NRC Nuclear Waste Geochemistry '83, US Nuclear Commission Report NUREG/CP-0052*.

Arzamastsev, A.A., Belyatsky, B.V., and Arzamastseva, L.V. (2000) Agpaitic magmatism in the northeastern Baltic Shield: a study of the Niva intrusion, Kola Peninsula, Russia. *Lithos*, **51**, 27–46.

Aslaner, M. and Kolaylı, H. (1996) Kop ultramafitlerinin paleojeotektonik konumuna analitik bir yaklasim. *KTU 30th Year Symposium*, Turkey (in Turkish).

Bektas, O. (1981) Kuzey Anadolu Fay Zonunun Erzincan-Tanyeri Bucağı yoresindeki jeolojik ozellikleri ve yerel ofiyolitik sorunları. PhD thesis, KTU, Turkey (in Turkish).

Bektas, O. (1982) Tanyeri (Erzincan) ofiyolitli karisigina ait trondhjemitlerin paleotektonik konumu ve kokenleri. *KTU Yerbilimleri Dergisi*, **2**, 39–50 (in Turkish).

Bektas, O., Pelin, S., and Korkmaz, S. (1984) Dogu Pontid yay gerisi havzasinda manto yukselimi ve polijenetik ofiyolit olgusu. *Ketin Symposium Proceedings*, pp. 175–188 (in Turkish).

Birsoy, R. (2002) Activity diagrams of zeolites: implications for the occurrences of zeolites in Turkey and of erionite worldwide. *Clays and Clay Minerals*, **50**, 136–144.

Bodinier, J.L. (1988) Geochemistry and petrogenesis of the Lanzo peridotite body, Western Alps. *Tectonophysics*, **149**, 67–88.

Buket, E. and Ataman, G. (1982) Erzincan-Refahiye ultramafik ve mafik kayaçlarının petrografik ve petrolojik özellikleri, *Yerbilimleri*, **9**, 5–18 (in Turkish).

Chipera, S.J. and Apps, J.A. (2001) Geochemical stability of natural zeolites. Pp. 81–161 in: *Natural Zeolites: Occurrence, Properties, Applications* (D.L. Bish and D.W. Ming, editors). Reviews in Mineralogy and Geochemistry, **45**. Mineralogical Society of America and the Geochemical Society, Washington D.C.

Coleman, R.G. (1977) *Ophiolites: Ancient Oceanic Lithosphere?* Springer-Verlag, New York.

Filippidis, A., Godelitsas, A., Charistos, D. and Tsipis, C. (1996) Natrolite/thomsonite intergrowths in basaltic rocks of Deccan Traps (Western India). *Neues Jahrbuch für Mineralogie-Monatshefte*, **4**, 161–170.

Flohr, M.J.K. and Ross, M. (1990) Alkaline igneous rocks of Magnet Cove, Arkansas: mineralogy and geochemistry of syenites. *Lithos*, **26**, 67–98.

Graham, I.T., Pogson, R.E., Colchester, D.M. and Baines, A. (2003) Zeolite crystal habits, compositions, and paragenesis, Blackhead Quarry, Dunedin, New Zealand. *Mineralogical Magazine*, **67**, 625–637.

Gunter, M.E., Knowles, C.R. and Schalck, D.K. (1993) Composite natrolite-mesolite crystals from the Columbia River Basalt Group, Washington. *The Canadian Mineralogist*, **31**, 467–470.

Hay, R. (1966) Zeolites and zeolitic reactions in sedimentary rocks. *Geological Society of America Special Paper*, **85**, 1–130.

Hay, R. (1980) Zeolitic weathering tuffs in Olduvai Gorge, Tanzania. Pp. 155–163 in: *Proceedings of the Fifth International Conference on Zeolites* (L.V. Rees, editor). Heyden, London.

Ibrahim, K. (1996) Geology, mineralogy, chemistry, origin and uses of the zeolites associated with Quaternary tuffs of Northeast Jordan. PhD thesis, University of London, UK.

Ibrahim, K. (2004) Mineralogy and chemistry of natrolite from Jordan. *Clay Minerals*, **39**, 47–55.

Ibrahim, K. and Hall, A. (1996) The authigenic zeolites of the Aritayn Volcanoclastic Formation, north-east Jordan. *Mineralium Deposita*, **31**, 514–522.

Irvine, T.N. and Baragar, W.R.A. (1971) A guide to the chemical classification of the common volcanic rocks. *Canadian Journal of Earth Sciences*, **8**, 523–548.

Kolaylı, H. (1996) Geological, petrological and metallogenic investigations of ultramafic and mafic rocks of Kop Mountains (Erzincan, Erzurum and Bayburt). PhD thesis, KTU, Turkey (in Turkish).

Langella, A., Cappelletti, P., and dé Gennaro, M. (2001) Zeolites in closed hydrologic systems. Pp. 235–259 in: *Natural Zeolites: Occurrence, Properties, Applications* (D.L. Bish and D.W. Ming, editors). Reviews in Mineralogy and Geochemistry, **45**. Mineralogical Society of America and the Geochemical Society, Washington D.C.

Lo, H.J. and Song, S.R. (2000) Factors controlling the distribution of zeolites in the andesitic rocks of the Central Coastal Range of eastern Taiwan. *Terrestrial Atmospheric and Oceanic Sciences*, **11**, 501–514.

Musaoglu, A. (1987) Kop-Gumushane yoresi jeolojisi ve maden prospeksiyonu raporu. *MTA Raport No: 8541*, Turkey (in Turkish).

Pearce, J.A. (1982) Trace element characteristics of lavas from destructive plate boundaries. Pp. 525–548 in: *Andesites* (R.S. Thorpe, editor). Wiley, New York.

Pearce, J.A., Harris, N.B.W., and Tindle, A.G. (1984) Trace elements discrimination diagram for the tectonic interpretation of granitic rock. *Journal of Petrology*, **25**, 956–83.

Prinzhofer, A. and Allegre, C.J. (1985) Residual peridotites and the mechanisms of partial melting. *Earth and Planetary Science Letters*, **74**, 251–265.

Ross, M., Flohr, M. and Ross, D. (1992) Crystalline solution series and order-disorder within the natrolite mineral group. *American Mineralogist*, **77**, 685–703.

Rouse, R.C., Dunn, P.J., Grice, J.D., Schlenker, J.L. and Higgins, J.B. (1990) Montesommaite $(K,Na)_9Al_9Si_{23}O_{64}.10H_2O$: a new zeolite related to merlinoite and the gismondine group. *American Mineralogist*, **75**, 1415–1420.

Schroeder, I., Thomson, G., Sulanowska, M. and Ludden, J.N. (1980) Analysis of geological materials using an automated X-ray fluorescence system. *X-ray Spectrum*, **9**, 198–205.

Schüssler, U., Richter, P. and Okrusch, M. (1989) Metabasites from the KTB oberpfalz target area, Bavaria geochemical characteristics and examples of the mobile behavior of 'immobile' elements. *Tectonophysics*, **157**, 135–148.

Sheppard, R.A. and Hay, R.L. (2001b) Formation of zeolites in open hydrologic systems. Pp. 261–275 in: *Natural Zeolites: Occurrence, Properties, Applications* (D.L. Bish and D.W. Ming, editors). Reviews in Mineralogy and Geochemistry, **45**. Mineralogical Society of America and the Geochemical Society, Washington D.C.

Sheppard, R.A. and Hay, R.L. (2001b) Occurrence of zeolites in sedimentary rocks. Pp. 217–233 in: *Natural Zeolites: Occurrence, Properties, Applications* (D.L. Bish and D.W. Ming, editors). Reviews in Mineralogy and Geochemistry, **45**. Mineralogical Society of America and the Geochemical Society, Washington D.C.

Teertstra, D.K. and Dyer, A. (1994) The informal discreditation of doranite as the magnesium analogue of analcime. *Zeolites*, **14**, 411–413.

Utada, M. (2001a) Zeolites in hydrothermally altered rocks. Pp. 305–322 in: *Natural Zeolites: Occurrence, Properties, Applications* (D.L. Bish and D.W. Ming, editors). Reviews in Mineralogy and Geochemistry, **45**. Mineralogical Society

of America and the Geochemical Society, Washington, D.C.

Utada, M. (2001b) Zeolites in burial diagenesis and low-grade metamorphic rocks. Pp. 277−303 in: *Natural Zeolites: Occurrence, Properties, Applications* (D.L. Bish and D.W. Ming, editors). Reviews in Mineralogy and Geochemistry, **45**. Mineralogical Society of America and the Geochemical Society, Washington, D.C.

Vattuone de Ponti, M.E. and Latorre, C.O. (1990) Low-grade metamorphism in granitoids and volcanic rocks, Cordillera Neuquina, Argentina. *Journal of South American Earth Sciences*, **3**, 247−252.